Video Technique for Measuring Dynamics of Liquid-Liquid Dispersion During Phase Inversion

A. W. Pacek, I. P. T. Moore, and A. W. Nienow
School of Chemical Engineering, University of Birmingham, Birmingham, B15 2TT, U.K.

R. V. Calabrese
Dept. of Chemical Engineering, University of Maryland, College Park, MD 20742

Studies on the dynamics of phase inversion available offer limited information due to the difficulty of following the transient mean and drop-size distribution. A new technique developed provides such data. A stereo microscope with a very shallow depth of field attached to a video camera gives sharp images of droplets in intensely-agitated, immiscible liquid dispersions by using a Strobotach pulsing at the camera framing rate. Droplets from 40 μm upward at concentrations up to 70% by volume dispersed phase can be measured accurately. Droplets of continuous organic phase in aqueous drops can be seen. The pictures can be analyzed semiautomatically using a computer and in-house software to give, using a variety of discretizations, cumulative and frequency distributions to any base and any mean size. Means and distributions are a function of time for phase inversions generated in three ways. The technique gives a powerful tool for understanding fast, complex dispersion processes.

Introduction

When a small amount of an immiscible oil phase is added to an aqueous one and the system is agitated, the oil becomes dispersed as oil drops. Addition of oil to give an ever increasing proportion eventually leads to the system becoming unstable at a certain high concentration of oil. This instability gives rise to dispersion of water in oil, that is, phase inversion occurs. Conversely, starting with a small amount of water in oil eventually leads to the opposite inversion. Much work has been conducted in trying to determine the composition (phase boundaries) at which inversion occurs. It has been found that the composition depends on a number of features, for example, the physical properties of the dispersed phases (Selker and Sleicher, 1965), the fluid dynamic conditions (Luhning and Sawistowski, 1971), the surface of the equipment (Kumar et al., 1991), and the presence of additives (Brooks and Richmond, 1991). In stirred reactors, a simple rule of thumb (Chapman and Holland, 1966) for pure liquids is that the phase which is present at less than about 0.3 volume fraction will be the dispersed phase. This rule leaves a large region between these two 0.3 volume fraction extremes where either phase may be dispersed called the ambivalent region.

In many operations, knowledge of which phase is dispersed is very important, for example, in mixer/settlers, while settling is generally very rapid for oil in water systems, it is much slower for water in oil (Kato et al., 1991). Thus, spontaneous inversion can be disastrous for the throughput of such equipment, and what causes the inversion is not well-known. Alternatively, under stable operating conditions, a step change in speed can deliberately trigger phase inversion and this may produce a desired product. For example, after phase inversion, the dispersed drops are often much smaller and, especially in the presence of surface active agents, this inversion may give rise to a stable product emulsion (Friberg, 1976).

The understanding of phase inversion is still extremely poor, especially in stirred vessels as pointed out in a recent review by Davies (1992), even though the phenomenon has been studied at intervals for about 40 years (Roger et al., 1956). Relatively recently, Gilchrist et al. (1989) proposed that the measurement of the delay time associated with phase inversion might provide a useful way of gaining insight into the dynamics of the process. In their experiments, the system was set up to take advantage of the two rules of thumb; first, the one dis-

Correspondence concerning this article should be addressed to A. W. Nienow.

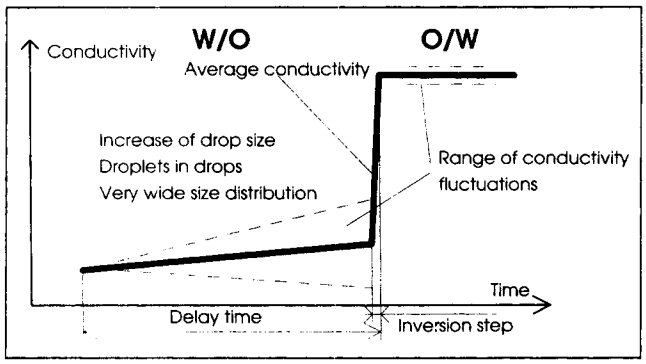

Figure 1. Dynamic conductivity trace as an aqueous phase dispersed in an immiscible oil inverts to oil in water.

cussed above and secondly, that the phase in which the impeller is placed will be the continuous one. Thus, using a concentration of chlorobenzene of about 40% by volume, with an impeller placed in it, led initially to a water in oil (w/o) dispersion (second rule of thumb) which after a certain period (the delay time, t_d), inverted to o/w (first rule of thumb). Gilchrist et al. (1989) also observed that over a quite narrow concentration range, t_d varied from zero (instantaneous inversion or one in which a w/o dispersion never formed) to infinity (w/o was always the stable structure). The delay time depended on a variety of fluid dynamic features (agitator speed, baffling, up or downward pumping) and liquid physical properties but could not be predicted *a priori*.

Gilchrist et al. (1989) used the measurement of conductivity (low values for w/o to high for o/w dispersions) to detect the phase inversion. A typical example of the transient conductivity response is shown in Figure 1. The process was also followed by a rather crude video system. The conductivity trace and video suggested that the final catastrophic instability represented by the very rapid transient response took place over a few seconds. During this time, a significant number of very large drops (up to 2 mm) formed. It also appeared that droplets of the continuous oil phase formed within these large water drops. After inversion, the drop size appeared to become much smaller. Since the article by Gilchrist et al. (1989), it has also been shown that under certain circumstances phase inversion does not occur if the agitator is started at very high speed. However, phase inversion will occur after a reduction from that speed, again with a delay time (Nienow et al., 1994). In other cases, for example, the reverse occurs, that is, no inversion at low speed with inversion after a delay time at high speed. Other recent work (Pacek et al., 1993) has also shown that the delay time depends on the physical properties of the two phases, and on the presence and concentration of additives which affect interfacial characteristics. Thus, the delay time depends on the same set of parameters as the phase boundaries.

For a given set of conditions, t_d is moderately reproducible to within about 5 to 10%. However, for a t_d of say 100 s, the $\pm 10\%$ variability is much greater than the 2 to 3 s of the final rapid transient. This poses a real problem for some size measurement techniques as discussed below.

Though it is often assumed that it is enhanced coalescence of the dispersed phase compared to its breakup (Arashmid and Jeffreys, 1980) that leads to phase inversion, we postulate that breakup of the continuous phase must also occur at this time. However, the possibility of the latter mechanism has been ignored. If the dynamic phase inversion experiments are to provide insight into the relative importance of these two mechanisms, it is clearly a major advantage if the full drop-size distribution can be followed throughout. This need to follow the full distribution was also pointed out by Davies (1992), and a good example of its value for the application of population balance concepts to the coalescence process has recently been published (Calabrese et al., 1993).

The technique reported here has been designed to enable the change of drop-size distribution and mean drop size to any base to be followed continuously and accurately during the whole delay time, including the final catastrophic transient. It should also be capable of confirming the presence of droplets within drops and of quantifying them in a similar way. Such measurements have never been conducted previously.

Characteristics of a Desired Size Measurement Technique vs. Those Currently Available

The main features of a dynamic phase inversion that present problems for a measurement technique designed to give the full size distribution are:

(1) That it occurs in highly concentrated dispersions (normally more than 60% dispersed phase).

(2) That it is difficult to predict exactly when it happens.

(3) That it involves very wide-size distributions and includes droplets-in-drops.

(4) That it often occurs rapidly and the final transient only takes a few seconds.

During the last two decades, several drop-size measurement techniques have been developed or adapted to drop-size measurements from particle-size measurements. In a recent review, Bae and Tavlarides (1989) discussed the operating range of each of these techniques in terms of dispersed-phase fraction (ϕ_d) and the ability to measure size distribution and minimum drop diameter (size resolution), though time resolution was not considered. They also pointed out the limits of their applicability. Most of these techniques were employed to measure the drop-size distribution (or mean drop size) in lean dispersions ($\phi_d < 5\%$) in carefully designed experiments. These experiments were aimed at supplying the data necessary to provide correlation constants for semi-empirical theories (or to develop empirical correlations) for mean drop diameter, and/or breakage/coalescence rates. Such experiments were performed either under steady-state conditions; or transient ones following a step change in agitator speed. However, even in the latter case, the crucial moment of interest was known *a priori*; and the degree of change of the mean drop size could be roughly predicted.

Clearly, none of the systems that have been developed meet all the requirements set out above. The need to have a full-size distribution will be further justified in the discussion section. However, the main limitation on the above list is the unknown moment of interest. This requires continuous measurement over a very long period of time. Any technique based on sampling will drastically change the overall composition of the dispersion unless recycling is used. If recycling were to be used, it would still alter the process under study and especially

the local composition at the point where the dispersion is returned to the vessel. The extreme sensitivity of delay time and phase inversion to composition (Gilchrist et al., 1989) clearly rules out this technique. Additionally, "physical" sampling of the dispersion with a wide drop-size distribution would require large sampling times, unsuitable to a rapid transient; and even then, the representativeness of the sample would be questionable (see Bae and Talvarides (1989) for a discussion of the influence of the capillary diameter on the accuracy of drop-size distribution measurements). These requirements practically eliminate all methods which involve sampling, including the capillary technique whichever method is used to convert drop lengths into the sizes of equivalent spheres. It is perhaps worth noting that a 10:1 size range of spherical drops requires a 1,000:1 difference in length to be measured by a capillary technique.

The only other techniques are photographic. With the standard camera, the need for frequent monitoring is still a major problem. However, by replacing the standard camera with a video camera, this limitation can be successfully overcome. The major disadvantages are that at volume fractions of dispersed phase greater $\sim 5\%$, observation is limited to the wall region, and that it also requires a light source in the vessel. It can be argued that: (a) the source of light can considerably alter the process; and (b) that the drop sizes close to the wall are not representative for the whole vessel. The first point will be discussed in detail in the next section. For the second point, estimates from the literature of coalescence rates (Muralidhar and Ramkrishna, 1986) compared to circulation times suggest that the latter are generally significantly faster than the former; and indeed, such arguments are used to justify the common assumption that stirred vessels can be modeled as perfectly mixed systems. This model means that *all spatial gradients equal zero*: the drop-size distribution is not a function of position. Given the other problems, it was decided that this limitation should be accepted for the present.

In this article, we present in detail for the first time a versatile and accurate video technique which has been applied successfully to the measurement of transient drop-size distribution during phase inversion, and the results are discussed below. The advantages and disadvantages of the technique will be discussed as well as means of enhancing its capabilities.

Video Measurement Technique

The video technique can be conveniently divided into two parts: the data acquisition and the data processing system. To fulfill the requirements set out above, a novel approach in both areas has been adopted. The data acquisition system consists of a high resolution video camera combined with a low magnification stereo microscope, a super VHS video recorder and a stroboscopic lighting system. This arrangement supplies high quality pictures of the dispersion essentially continuously over any period of time. By a proper choice of the magnification and the focal length, both small (40 μm) and large drops (2,000 μm) can be measured as well as the structure of the dispersion, that is, the presence of droplets-in-drops.

Even though the quality of the pictures produced by such a system is very high, the commercially available image analyzing packages for data processing are not able to analyze the pictures automatically. This inability is because of the very high proportion of overlapping drops and the need to distinguish droplets-in-drops, as well as specifying which drop belongs to each phase. It is also desirable to be able to calculate the characteristics of the distribution, that is, frequency and cumulative distributions to different bases and different mean drop diameters. Software has also been developed which can handle all of these features semiautomatically and is described in detail in the next section.

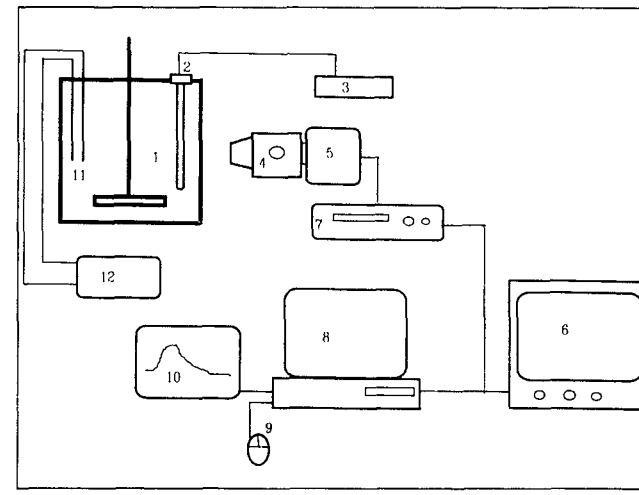

Figure 2. Experimental apparatus.

(1) Stirred vessel; (2) strobe lamp; (3) strobe flash; (4) low magnification stereo microscope; (5) video camera; (6) TV monitor; (7) video recorder; (8) PC 486 computer with digitizing system; (9) mouse; (10) printer; (11) conductivity probe; (12) conductivity meter.

Technical description

The mixing equipment in which phase inversion was investigated and the associated video measurement system are shown in Figure 2. A Panasonic model WV-F15 video camera with 400 lines resolution was mounted on a low magnification Olympus model SZ 6045 TR zoom stereo microscope. The microscope had magnification ratios of 20 to 110 times actual size at focal distances of 15 to 80 mm, respectively. The resulting depth of field was less than 2 mm and decreased with increasing magnification. The camera has a framing rate of 50/s and during recording or playback, two adjacent frames are usually superimposed so that the information displayed on the video monitor changes every 1/25th s. In this application, a Panasonic model AG 7355 high resolution, super VHS format, video recorder with digitizing facilities was employed with a Sony model KV 1440 UB, 340 mm diagonal, color monitor. The digital capability allowed the individual frames to be separated so that a single frame of information for each 1/50th s interval can be displayed.

In addition, the camera is equipped with a high speed shutter capable of capturing from 1/120th to 1/2,000th s of information per frame. In this high speed shutter mode, light is intermittently passed to the video camera so that each frame contains information of a more discrete event than the 1/50th s framing rate. This facility allows capture of higher speed events with greater clarity than with the standard shutter speed. However, in monitoring liquid-liquid dispersions at typical

agitation rates, it was found that sufficient clarity could not be obtained using the high speed shutter mode alone. Therefore, light is provided using a Dawe Transistor type 120900 Strobotach whose pulsing frequency is synchronized with the camera framing speed, that is, the flashing rate was set to 50/s. Since the flash duration of the strobe is small compared to the shutter opening time, discrete frozen events are captured providing sharp images. Depending upon the application, the Strobotach is employed with the camera in the normal operating mode or in the high speed shutter mode. In the latter mode, a trial and error procedure is employed, while viewing the dispersion on the monitor, to select the shutter speed that gives the highest image quality.

A strobo-slave lamp is placed in a 1-cm-dia. glass well that is inserted into the vessel. The gap between the inside of the vessel wall and the front of the lamp well can be varied from 2 to 8 mm. The vertical position of the well can also be varied so that data can be acquired at almost any height (except within a few millimeters of the vessel top or bottom). The influence of the strobe well on phase inversion was checked by measuring the delay time with the conductivity probe for the same system with the strobe well present in the vessel and when it was removed. It has been found that the delay time was the same within the accuracy of the experiment. It is reasonable to conclude that other aspects of the phase inversion, that is, the change of drop-size distribution, are the same too.

After the video pictures have been acquired, the event is played back on the monitor to qualitatively observe the results and to select individual frames for digitization. Each frame is sent to a Tandon 486 SX personal computer. Digitization is accomplished using a Rambo Vidi PC interface board with version 2.1 software. After digitization, pictures can be printed using a HP Laser Jet 4 printer; see examples below. Extending the interface board memory to 120 KB enables reproduction of either black and white or color images of the dispersion on the computer monitor. The software also allows enhancement of contrast and color. Although a high quality image is produced, it is still too complex to be readily analyzed by a fully automated technique as discussed above.

Software was developed within Windows 3.1 to measure the size of spherical drops. A mouse is used to place three points on the perimeter of each drop. This software then inserts a triangle connecting these points, thus indicating that the local point coordinates are stored in the computer memory. This action also ensures that the last three entries are associated with the drop being analyzed and prevents the same drops from being counted more than once. The drop diameter is then calculated, in pixels, from the coordinates of the inscribed triangle. In the experiments described later, the number of in-focus drops per frame varied from 20 to 120 and the analysis time ranged from 1 to 8 min per frame. The software can be modified to accommodate nonspherical drops, though within the results presented here that was not necessary. Furthermore, various colors can be selected for the marker points. Therefore, by selecting two or more colors, it is possible to modify the software to extract simultaneously two or more size distributions from a single experiment, for example, when continuous phase droplets are contained within dispersed-phase drops.

After digitization, drop diameters, measured in pixels, are stored for each frame in a separate ASCII file. The diameter is next recalculated to microns using a calibration curve or correlation obtained by videotaping a 1.00-mm-dia. wire throughout the magnification range of the microscope. The resolution depends on the magnification and, in the current equipment, can be varied from 4 to 24 μm per pixel. A Fortran program reads the data from the ASCII files and calculates different mean diameters and distribution functions to different bases and to different discretization modes. The latter term refers to the way in which discrete size classes for determination of probability density functions or other distribution measures are specified. For instance, the data can be placed in bins of equal width or bins of variable width based on, for example, geometric or Fibonacci (Chang et al., 1991) series. The nominal diameter for each size class is then taken as the arithmetic average of the bin cutoff diameters.

Quality of pictures

The detailed description of the phase inversion experiments is given later. Within this section on the technique, pictures that were taken from those experiments in which water/glycerol (GW) (aqueous phase) was dispersed in chlorobenzene (CLB) are used to validate the system.

Figure 3 shows two examples of the pictures available. Figure 3a is a digitized "dump" of the screen image used for data processing, and Figure 3b is a still frame taken from the videotape by a Sony UP-3000P video printer. The picture quality is good, that is, the drops have sharp edges and are easy for the human eye to assess. Even so, they confirm the difficulty of handling them automatically by computer as discussed above. The main dispersion at this stage consists of drops of GW dispersed within CLB, and these GW drops range in diameter from around 100 to 2,500 μm. However, within almost all the GW drops, there are CLB droplets ranging from a few tens to a few hundreds of microns. In some cases, the packing of CLB droplets in the GW drops is very high.

Thus, Figure 3 shows the wide range of drop size that the technique is capable of measuring, and also the ability to detect droplets-within-drops.

Accuracy of measurements

There are two sources of error which can arise while measuring drop size that must be taken into account. They are associated with:

(a) Sizing drops which are out of focus.

(b) Placing the cursor on the drop perimeter.

In the first case, the magnification ratio for a drop which is in focus is different from that for one that is out of focus. Simple tests performed with the calibration wire show that if the operator is careful and only the drops which are reasonably in focus are measured, then the difference in magnification can be kept to within $\pm 5\%$.

The error resulting from placing the cursor (the second case) is a simple consequence of the resolution of the human eye. The actual picture consists of pixels and the computer screen used here has a total size of 512 by 512 pixels. The physical size of the picture on the screen is 120 by 120 mm and the human eye, when the operator is sitting in front of the screen, can reasonably distinguish $+/-0.5$ mm, that is, 2 to 3 pixels. The thickness of the drop perimeter is about the same size (at high magnification), so the drop diameter can be measured to within an accuracy of 2 to 4 pixels. This, expressed in microns,

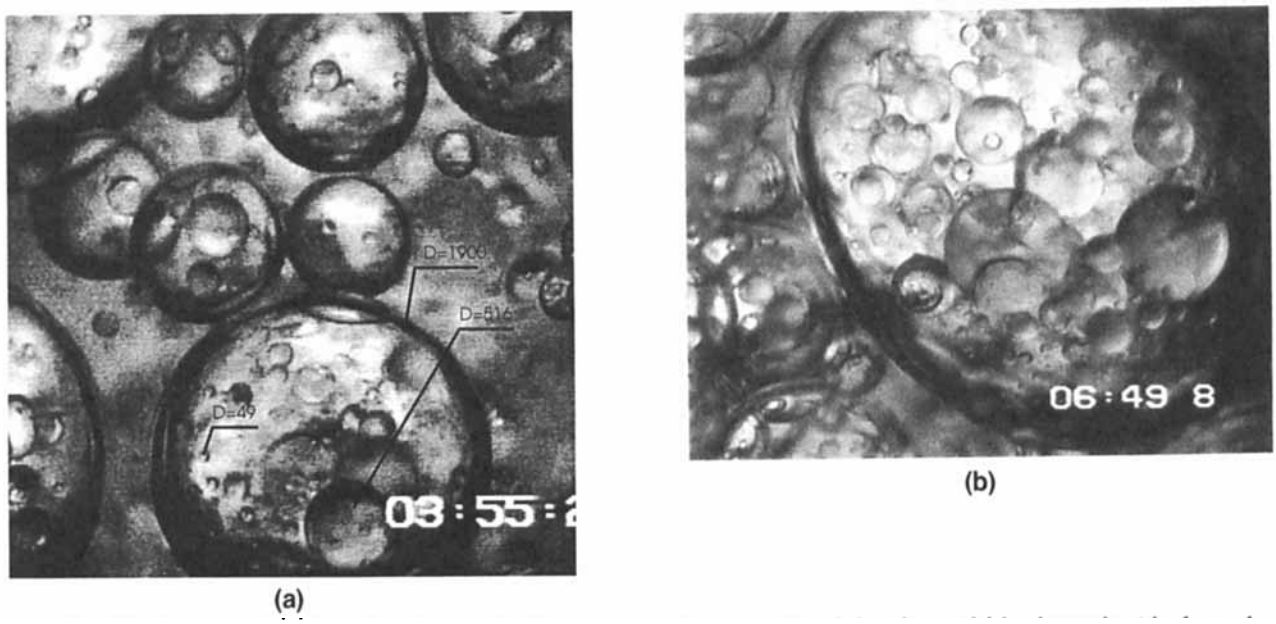

Figure 3. Structure of glycerol/water drops dispersed in chlorobenzene and droplets-within-drops just before phase inversion.

(a) "screen dump" (D represents size of drops in μm); (b) print from the Sony video printer. (Time given represents period from start of experiment-phase inversion after 7 min 10 s.)

means that at high magnification the resolution is between 8 to 16 μm; and at low magnification it is between 25 to 90 μm. Therefore, the smallest drops which have been analyzed to date, keeping the absolute accuracy to within 10% to 20%, were of the order of 40 μm. However, a higher magnification model of the microscope used here is available and can be incorporated into the system.

Number of drops to provide a representative sample

To minimize the time required for the analysis of one population of drop sizes, it is desirable to measure as few drops as possible. However, the number must be sufficient to give a representative sample and this number must be assessed. Therefore, populations were analyzed from two types of experiments: a phase inversion, as reported here, and coalescence following a reduction in agitator speed in a dilute dispersion. Data for the latter case are not presented here. The validation procedure was the same in both cases. Starting from a relatively small sample (200 drops), the number of drops was gradually increased incrementally up to around 2,000 drops in the phase inversion experiment and 1,300 in the coalescence experiment. For each sample, drops were assigned to prescribed bins and a range of mean diameters was calculated from:

$$D_{pq} = \left[\frac{\Sigma n_i D_i^p}{\Sigma n_i D_i^q} \right]^{1/(p-q)} \tag{1}$$

as well as the volume and number density functions. (Though the facility for discriminating droplets-in-drops as indicated in the description of the video system is available, it was not used here. Therefore, all drops counted were considered to be part of the same distribution. Such an assumption makes little difference to the higher moments, because all the large drops are drops of water. However, many of the smaller drops are droplets of CLB in the water drops. Their inclusion in D_{10} certainly affects it. Further consideration is required of how such systems should be accommodated in calculating mean and size distributions. Clearly, this video technique makes this possible but the point is not further developed here.) As an example, the mean drop diameters are shown in Figure 4a and volume density distributions in Figure 4b for different sample sizes. The size of the sample was accepted as representative when the difference in mean diameters calculated from two consecutive samples was smaller than 5% (Figures 4a). With more than this number of drops in the sample, the volume density distributions, which are the most sensitive, virtually overlap (Figure 4b).

Although the ratio of the maximum to the minimum drop diameters were different ($\simeq 40$ for phase inversion and 20 for coalescence); and one was bimodal (coalescence) and the others unimodal (phase inversion), the number of drops above which consistent mean size and distribution functions resulted was roughly the same. Therefore, it was concluded (see Figure 4) that a sample population should not be smaller than 800 drops. To obtain this population, between 8 to 40 frames are required. All can be acquired within a second or so since 25 pictures per s (or 50 frames after splitting) are produced. However, it should be noted that even at this framing rate, it was extremely rare to find the same drop in consecutive frames. This aspect became clear when trying to follow the same "droplets-within-drops" structure. Thus, double counting rarely, if ever, occurs. Calculations based on drops moving at 10% of the impeller tip speed lead to the same conclusion.

Experiments

General procedure and physical data

The experiments were conducted in a 15-cm-ID cylindrical,

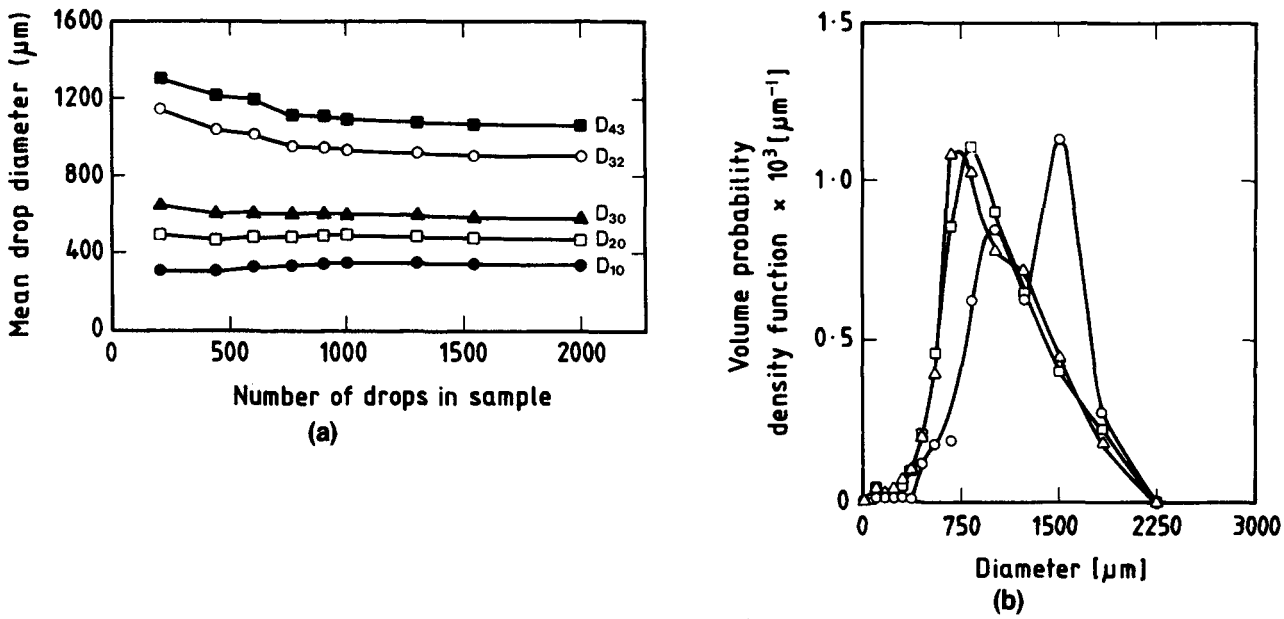

Figure 4. Data from a phase inversion experiment to show the effect of the sample size on (a) mean drop diameter; (b) volume probability density function (for size classes based on a geometric series ratio $\sqrt{2}$).

(○ = 200 drops; △ = 800 drops; □ = 1,300 drops.)

flat-bottom glass tank equipped with 4 equally spaced stainless steel baffles of 1.5-cm width, and a 60° pitch, 4 blade turbine of 7.5 cm diameter was placed 25 mm off the tank bottom (Figure 2). The vessel was placed inside a square, water-filled jacket with optically flat glass sides that also served as a constant temperature bath and allowed video monitoring through the cylindrical tank wall with minimal optical distortion. All stainless steel parts in contact with the liquids were polished to maximize cleanliness, and the latter was maintained by a rigorous procedure based on thorough cleaning followed by soaking with Decon and distilled water washing. The motor shaft entered through a sealed bearing which was further water jacketed so that high impeller speeds could be achieved without air entrainment. The tank was operated completely filled and the height of liquid in the tank was equal to the internal diameter.

The organic phase in the work reported here was always chlorobenzene (CLB). The aqueous phase was water or one of the following glycerol-water (GW) solutions: 1%, 10%, 25%, and 36%. The lowest glycerol concentration was chosen so that the density and viscosity of the solution were almost identical to those of water, while the interfacial tension of the solution with respect to chlorobenzene was significantly different from that for chlorobenzene/water. The interfacial tension does not change much with further increases in glycerol concentration, though the viscosity and density increase significantly. The highest concentration of glycerol was chosen so that the density of that aqueous phase was still lower than that of the organic phase. Thus, since the volume fraction of CLB used was 0.425, the impeller was always positioned in the organic phase. The actual physical properties of the liquids are given in Table 1. Interfacial tension was measured by the drop weight method and viscosity by a Contraves Rheomat 30. Density was taken from the literature (chlorobenzene) or measured with a density bottle (glycerol solutions).

Carefully measured amounts of liquids were charged into the vessel keeping the volume fraction of CLB at 0.425 and the system was left to equilibrate at the temperature of 20°C. Great care was taken to remove all air from the vessel and to ensure that, during the run, none entered. This precaution was taken because earlier work (Gilchrist et al., 1989) showed that air bubbles had a profound effect on the delay time. The magnification (defined as the ratio of the diameter of the drop as seen on the TV monitor to the real size of the drop) of the microscope was chosen to suit the size distribution of the drops and, in most cases, it was between 70 and 100. The recording was begun before the impeller was started and the conductivity and the temperature of the dispersion was monitored and recorded on a two pen recorder. For each system, three experiments were conducted at each speed with the lowest speed being selected to ensure that visually the GW was fully dispersed in the CLB, that is, $N > N_{JD}$, the minimum impeller speed to ensure complete dispersion.

Table 1. Liquids Used in the Experiments

Liquids	Density (kg/m^3)	Viscosity (mPa·s)	Interfacial Tension ($N/m \times 10^2$) with CLB	Phase
Chlorobenzene (CLB)	1,106	0.75	—	Oil
Water	998.2	1.00	3.34	
1% glycerol in water	999.2	1.02	2.49	
10% glycerol in water	1,026.1	1.23	2.47	Aqueous
25% glycerol in water	1,063.1	2.02	2.67	
36% glycerol in water	1,085.0	3.10	2.61	

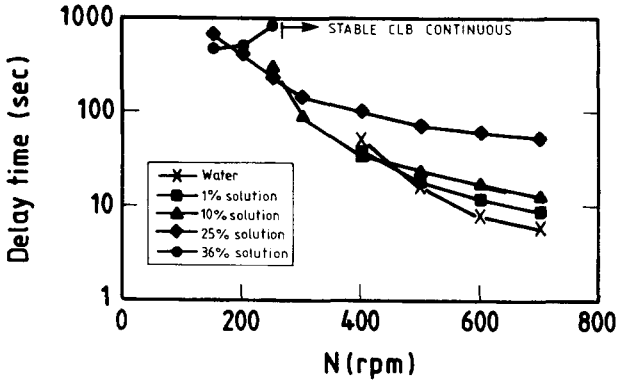

Figure 5. Delay time vs. impeller speed after starting from rest for the water/chlorobenzene and GW/CLB systems of Table 1.

Results

Spontaneous delay time studies

Phase inversion from aqueous phase dispersed (w/o dispersion) to oil phase dispersed (o/w dispersion) for water/CLB and for GW/CLB were investigated. All the systems studied were initially chlorobenzene continuous throughout the whole range of impeller speeds. Phase inversion then generally occurred after a certain delay time which depended on the impeller speed and increased with the increase of concentration of glycerol in water (see Figure 5). At 36% w/w glycerol, the system only inverted at speeds less than 300 rpm and above that became stable aqueous phase dispersed. In the last case, the phase inversion could be generated by reducing the impeller speed from greater than 300 rpm to lower speeds but greater than N_{JD}.

The increase of delay time (the increase of stability of the initial dispersion) can be ascribed to either the fall in interfacial tension, the increase of viscosity of dispersed phase or by the decrease of the density difference between the phases. However, discussion of which of the three parameters caused such a drastic change of the delay time (from a few seconds to infinity) is beyond the scope of this article and has been presented by Nienow et al. (1994).

Drop-size changes observed during phase inversion

The systems described above enabled phase inversion to be generated in three different ways:

(1) Spontaneous phase inversion after starting the impeller from rest, as shown in Figure 5.

(2) Phase inversion generated by a step increase of impeller speed.

(3) Phase inversion generated by a step reduction in impeller speed.

Examples of the change of drop-size distribution and mean drop size as a function of time is described below for each of these three cases.

The spontaneous phase inversion example is for the water/CLB system and the evolution of mean drop diameters and volume drop-size distribution with time using an arithmetic discretization are shown in Figures 6a and 6b, respectively.

The phase inversion example generated by increasing the impeller speed was for 25% GW/CLB. From Figure 5, it is clear that at an impeller speed of 150 rpm, this system inverted spontaneously after approximately 900 s. Therefore, initially liquids were mixed for 60 s at 150 rpm and, at that time, the impeller speed was increased stepwise to 450 rpm. The measured delay time following the change was 185 s which can be compared with the delay time of ~90 s (see Figure 5) when the impeller was started from rest. The evolution of the average drop diameters, and examples of the volume and number drop-size distributions both before and after phase inversion are shown in Figures 7a, 7b, and 7c, respectively. This time geometric discretization (ratio $=\sqrt{2}$) has been used.

The phase inversion generated by a step decrease of impeller speed used the 36% GW/CLB system. In this case, the impeller was started at 400 rpm, which gave a dispersion which was stable chlorobenzene continuous (see Figure 5). After 10 min of stirring, the impeller speed was decreased to 200 rpm and after 100 s, the system inverted to water continuous. Again, this delay time can be compared with a value of 650 s when stirring at 200 rpm starting from rest (see Figure 5). The ev-

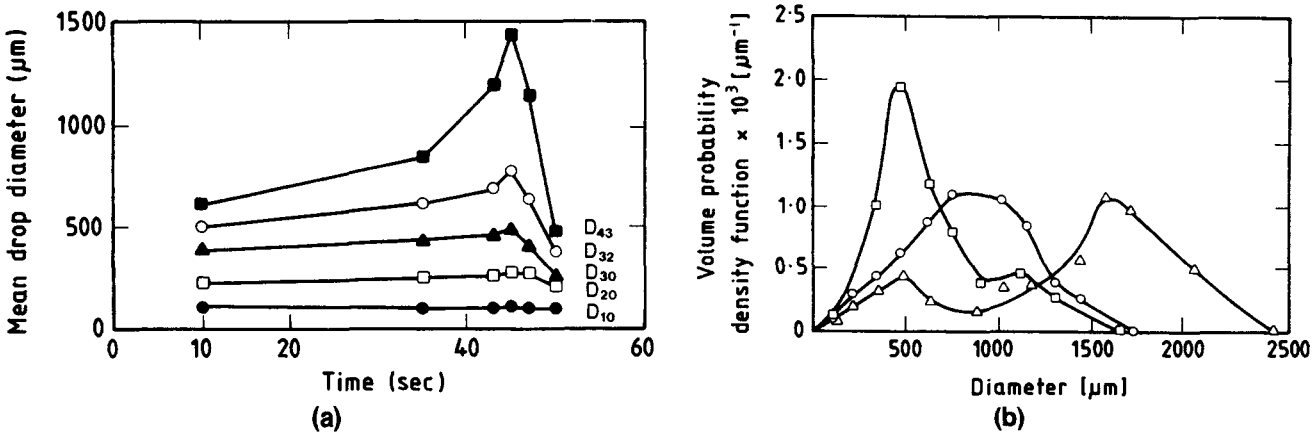

Figure 6. Spontaneous phase inversion from water dispersed in CLB to CLB dispersed; impeller started at 500 rpm with inversion after 45 s.

(a) mean drop diameters vs. time; (b) volume probability density functions: □ = after 10 s; ○ = after 35 s; △ = after 45 s during the final transient.

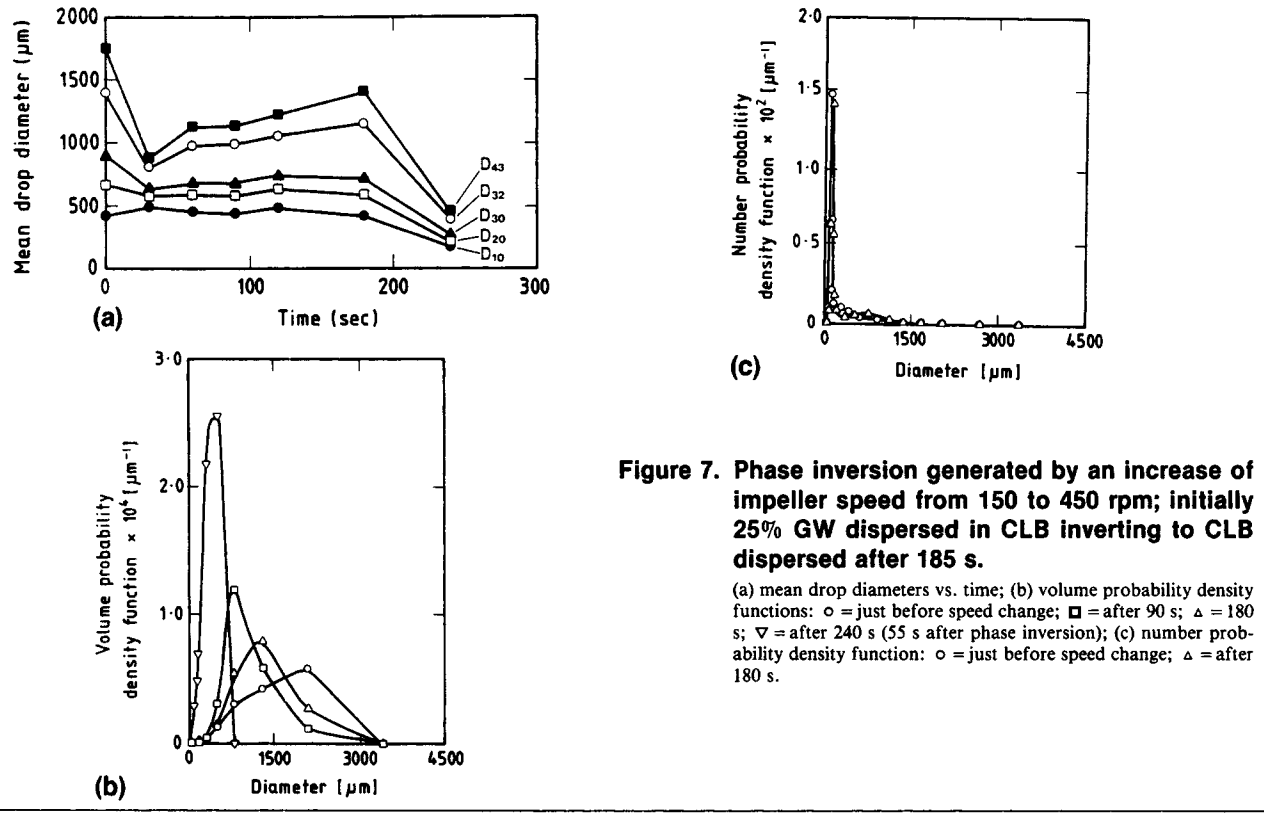

Figure 7. Phase inversion generated by an increase of impeller speed from 150 to 450 rpm; initially 25% GW dispersed in CLB inverting to CLB dispersed after 185 s.

(a) mean drop diameters vs. time; (b) volume probability density functions: ○ = just before speed change; □ = after 90 s; △ = 180 s; ▽ = after 240 s (55 s after phase inversion); (c) number probability density function: ○ = just before speed change; △ = after 180 s.

olution of the average drop diameters and the volume drop-size distribution are shown in Figures 8a and 8b respectively using arithmetic discretization.

Discussion

Present results

The detailed discussion of the mechanism of phase inversion is beyond the scope of this article, but the results shown above clearly indicate that whichever way the phase inversion is approached the behavior of the system is rather similar. In order to show that similarity, the full scope of the present technique is brought to bear, that is, the observations provided by the video pictures together with the full-size distributions and the means to any base.

This similarity can be expressed in the following way. There is an initial period in which all the mean drop sizes except d_{10} respond to the immediate change in impeller speed (except when starting from rest since sensible readings cannot be taken

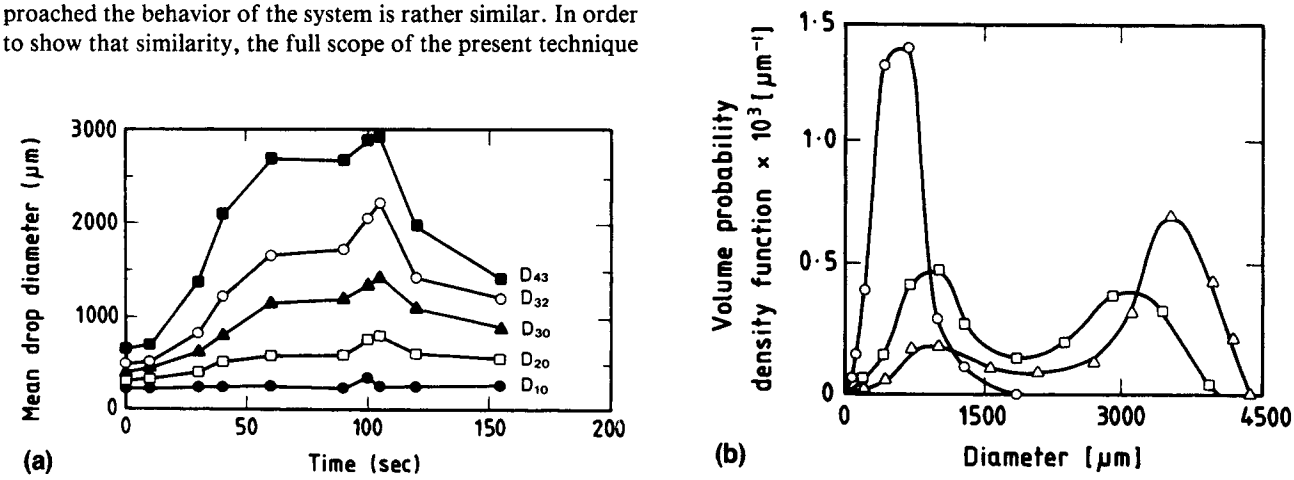

Figure 8. Phase inversion generated by a decrease of impeller speed from 400 to 200 rpm; initially 36% GW dispersed in CLB inverting to CLB dispersed after 100 s.

(a) Mean drop diameters vs. time; (b) volume probability density functions: ○ = just before speed change; □ = after 40 s; △ = after 100 s during final transient.

for about 10 s (Figure 6), as this time is considered to be about the minimum required to establish the dispersion). However, as would be expected, an increase in speed initially leads to a reduction in size (Figure 7) while a decrease leads to an increase in size (Figure 8). There is then a period during which steady growth appears (Figures 6a, 7a, and 8a), even for the case (Figure 7a) in which speed has been increased. Finally, there is a dramatic increase, especially in the higher moment diameters just before phase inversion occurs. This period corresponds with the marked increase of conductivity fluctuations (which can now be explained by the video observation of the very large drops) and the final conductivity transient indicated in Figure 1. During all this time, droplets of CLB appear in all but the smallest drops of water. Following phase inversion, the mean sizes always fall and droplets of water in drops of CLB are not seen.

There are also some differences in detail which the video technique draws out. For example, Figure 7b shows that the change of volume drop-size distribution following a speed increase to give phase inversion remains unimodal. Figure 8b, on the other hand, following the change arising from a speed decrease shows bimodal distributions as phase inversion is approached.

The higher the moments, the more influence the large drops have. However, the figures also show that these are still very large numbers of tiny drops with an exceedingly wide distribution. Figures 6b, 7b, and 8b which show the frequency distributions on a volume basis suggest that while there is a progressive increase in the larger drops, the size of the smallest drops does not change. Indeed, the frequency distribution on a number basis (Figure 7c) does not allow any interpretation to be made; and the small reduction in number mean, d_{10}, (Figures 6a, 7a, and 8a) suggests that the number of smaller as well as the number of larger drops is increasing during the period. However, in these figures, d_{10} is also influenced by the growing number of droplets within drops (as mentioned earlier). The combination of the two changes suggests that both breakup of the continuous phase to give droplets-within-drops (effectively decreasing the volume fraction of the continuous phase), as well as coalescence of the dispersed phase to give larger drops, are participating in the phase inversion process. Dispersed-phase coalescence has normally been considered the most important mechanism controlling phase inversion. The importance of continuous phase breakup (instability) as a parallel mechanism is a new contribution to the understanding of this complex process.

Droplets of continuous phase in drops of dispersed phase have also been discussed extensively by Brookes and Richmond (1991) for two immiscible phases heavily dosed with surfactant, but they have not considered the dynamics of their formation.

Other applications of present size analysis technique

Though not discussed here, this video technique is obviously applicable to other dispersed two-phase systems in other geometries. Thus, it is being used in our laboratory to study high concentration liquid-liquid breakup and coalescence processes in stirred vessels and pipes. The ease of collecting transient data also makes it ideal for solving the inverted population balance equation (Tobin et al., 1990). In addition, because of the completely different images generated by liquid droplets and gas bubbles, it is very easy to use in gas/liquid/liquid systems. An example is shown in Figure 9 where the dark circles are the air bubbles.

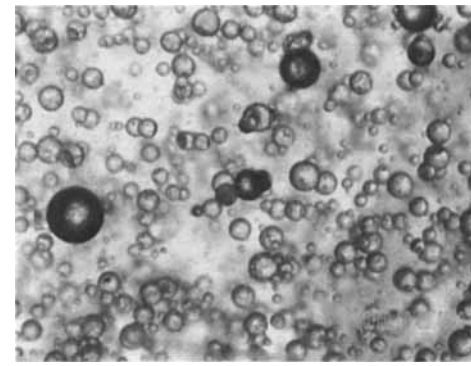

Figure 9. An example of the picture of a three-phase system.

5% CLB dispersed in water with some air bubbles present.

Summary and Conclusions

We have developed an accurate, versatile, and user-friendly video technique especially for the study of the rapid transients in mean and drop-size distribution that occur during phase inversions. The system has been validated by showing pictures and data sets. The major advantages are:

(1) The almost instantaneous capture of the drop-size distribution allows quantitative analysis of rapid transients.

(2) Continuous monitoring does not require *a priori* knowledge of the occurrence of critical events.

(3) Event details can be revisited or reanalyzed without repeating the experiment and used to provide more numerical data if necessary, or broadly confirm visually the data relating to that event.

(4) Droplets-within-drops can be analyzed.

(5) The microscope's zoom feature can be used to change magnification rapidly. This facility allows accurate monitoring of distributions whose size changes significantly with time; or a detailed analysis of the large and small tail of very broad distributions.

(6) Data reduction and analysis is integrated into the system and is therefore relatively rapid compared to standard photographic techniques.

The major disadvantages are:

(1) Data treatment is slower than for fully automatic techniques. However, other such techniques either only give a mean size, or are limited by their ability to capture a representative sample and disturb the system if operated continuously. The present system is designed to accommodate improved software to facilitate data analysis for high drop concentrations and such software is being developed.

(2) The present arrangement is limited to monitoring the wall region of a stirred vessel except for dilute dispersions. However, optical fiber systems, endoscopes, and advanced lighting techniques offer the potential for a spatially more versatile arrangement. This weakness is also being worked on and encouraging progress is being obtained.

Acknowledgments

We wish to express our thanks to BHR Group, ICI, and Unilever, our collaborators in this Biochemical Engineering LINK project and the U.K. Science and Engineering Research Council and Dept. of Trade and Industry for their financial support for it. R. V. Calabrese acknowledges support as a Fulbright Scholar and a U.K. SERC Visiting Fellow for his sabbatical stay at the University of Birmingham.

Notation

D_i = arithmetic mean diameter of the ith bin
D_{pq} = mean diameter defined by Eq. 1 formed from the pth and qth moments of the drop-size distribution
D_{10} = number mean diameter
D_{20} = area mean diameter
D_{30} = volume mean diameter
D_{32} = Sauter mean diameter
D_{43} = mass averaged diameter
n_i = number of drops in the ith bin
N = impeller speed
p,q = moments of drop-size distribution

Literature Cited

Arashmid, M., and G. V. Jeffreys, "Analysis of the Phase Inversion Characteristics of Liquid-Liquid Dispersions," *AIChE J.*, **26**, 51 (1980).

Bae, J. H., and L. L. Tavlarides, "Laser Capillary Spectrophotometry for Drop-Size Concentration Measurements," *AIChE J.*, **35**, 1073 (1989).

Brooks, W. B., and H. N. Richmond, "Dynamics of Liquid-Liquid Phase Inversion Using Nonionic Surfactants," *Colloids and Surf.*, **58**, 131 (1991).

Calabrese, R. V., A. W. Pacek, and A. W. Nienow, "Coalescence of Viscous Drops in a Stirred Vessel," *I. Chem. Res. Event*, Birmingham, U.K., published by IChE, Rugby, U.K., p. 642 (1993).

Chang, Y. C., R. V. Calabrese, and G. W. Gentry, "An Algorithm for Determination of the Size Dependent Breakage Frequency of Droplets, Flocs and Aggregates," *Part. Part. Syst. Charact.*, **8**, 315 (1991).

Chapman, F. S., and F. A. Holland, *Liquid Mixing and Processing*, Reinhold, New York, p. 208 (1966).

Davies, G. A., "Mixing and Coalescence Phenomena in Liquid-Liquid Systems," in *Science and Practice of Liquid-Liquid Extraction*, J. D. Thornton, ed., Vol. 1, Clarendon Press, Oxford, p. 245 (1992).

Friberg, S., ed., *Food Emulsions*, Marcel Dekker, New York (1976).

Gilchrist, A., K. N. Dyster, I. P. T. Moore, A. W. Nienow, and K. J. Carpenter, "Delayed Phase Inversion in Stirred Liquid-Liquid Dispersion," *Chem. Eng. Sci.*, **44**, 2381 (1989).

Kato, S., E. Nakayama, and J. Kawasaki, "Types of Dispersion in Agitated Liquid-Liquid Systems," *Can. J. Chem. Eng.*, **69**, 222 (1991).

Kumar, S., R. Kumar, and K. S. Gandhi, "Influence of the Wetting Characteristic of the Impeller on Phase Inversion," *Chem. Eng. Sci.*, **46**, 2365 (1991).

Luhning, R. W., and H. Sawistowski, "Phase Inversion in Stirred Liquid-Liquid Systems," *Proc. Int. Solvent Extraction Conf.*, Vol. 2, The Hague, published by Society of Chemical Industry, London, p. 873 (April 19-23, 1971).

Muralidhar, R., and D. Ramkrishna, "Analysis of Droplet Coalescence in Turbulent Liquid-Liquid Dispersions," *Ind. Eng. Chem. Fundam.*, **25**, 554 (1986).

Nienow, A. W., A. W. Pacek, I. P. T. Moore, and J. Homer, "Fundamental Studies of Phase Inversion in a Stirred Vessel," *Proc. Euro. Conf. on Mixing*, Instn. of Chem. Eng., Rugby, England, p. 171 (Sept., 1994).

acek, A. W., I. P. T. Moore, R. V. Calabrese, and A. W. Nienow, "Evolution of Drop Size Distribution and Average Drop Diameter in Liquid-Liquid Dispersions Before and After Phase Inversion," *Trans. I. Chem. E.*, Part A, **71**, 340 (1993).

Roger, A. W., V. G. Trice, and J. H. Rushton, "Effect of Fluid Motion on Interfacial Area of Dispersions," *Chem. Eng. Prog.*, **52**, 515 (1956).

Selker, A. J., and C. A. Sleicher, "Factors Affecting Which Phase Will Disperse When Immiscible Liquids Are Stirred Together," *Can. J. Chem. Eng.*, **43**, 298 (1965).

Tobin, T., R. Muralidhar, M. Wright, and D. Ramkrishna, "Determination of Coalescence Frequencies in Liquid-Liquid Dispersions: Effect of Drop Size Dependence," *Chem. Eng. Sci.*, **45**, 3491 (1990).

Manuscript received June 3, 1993, and revision received Dec. 22, 1993.